

A BIOMECHANICAL MODEL OF THE HUMAN CORNEA

UN MODELO BIOMECÁNICO DE LA CÓRNEA HUMANA

O. NÚÑEZ-CHONGO, C. MUÑOZ-VILLAESCUSA, A. J. BATISTA-LEYVA[†]

Instituto Superior de Tecnologías y Ciencias Aplicadas, Universidad de La Habana, 10400 La Habana, Cuba; abatista@instec.cu[†]

[†] corresponding author

Recibido 6/4/2018; Aceptado 6/6/2018

Numerical modeling of human cornea has paramount importance to test *in silico* surgical procedures and to understand the effect on human eyes of injuries and other external aggressions. To prepare a numerical model that could reproduce correctly corneal behavior, it is necessary firstly to select a type of elastic material and its mechanical model of response. Then a numerical procedure must be implemented; normally FEM is used for calculations. It is then necessary to select geometry, create a mesh and calculate the elastic constants of the model. In the present contribution we create a model based in Mooney Rivlin hyperelasticity, with a mesh consisting in three layers and eleven elements per meridian from the apex to limbus. Two geometries were tested: cornea fixed by limbus and a second one formed by cornea, corneal limbus and part of sclera. We also prepared and tested the numerical procedure for establishing the stress free configuration.

La modelación numérica del comportamiento de una córnea humana es importante para simular computacionalmente procedimientos quirúrgicos sobre esta, así como la acción de agentes externos agresivos. Un modelo numérico que reproduzca de manera fiel el comportamiento de la córnea debe basarse en un tipo de elasticidad del material que la compone. Las constantes del material se determinan ajustando el modelo a experimentos. A continuación se implementa un modelo numérico, basado por lo general en elementos finitos. Debe escogerse una geometría, las condiciones de frontera que se deben cumplir y una malla para discretizar las ecuaciones continuas. En este trabajo presentamos la creación de un modelo de córnea, basado en un material que cumpla las condiciones de material hiperelástico de tipo Mooney Rivlin, sustentado en una malla de tres capas y once elementos por meridiano (del ápice al limbo). Las geometrías utilizadas fueron una córnea fija por el limbo y una segunda formada por la córnea, el limbo y parte de la esclera. Se estableció el procedimiento para determinar la configuración libre de estrés de la córnea.

PACS: Biomaterials (Biomateriales), 87.85.J; physical properties of biomaterials (propiedades físicas de los biomateriales), 87.85.jc; finite element analysis (análisis de elementos finitos), 02.70.Dh

I. INTRODUCTION

The human cornea is a transparent membrane (a concave meniscus) responsible of two thirds (around +43 D) of the refracting power of human eyes [1]. This explains why cornea is a preferred zone for refractive surgery to correct myopia, hyperopia etc. At the same time any pathology or physical trauma affecting it has a repercussion in the optical quality of the eye. Cornea also works as a protective structure for inner tissues and intraocular humors [2]. Structurally, it is composed of proteins and well-structured cells, fed through tears and aqueous humor. Cornea could be divided in five distinct layers: Epithelium, Bowman's Membrane, Stroma, Descemet Membrane and Endothelium. Mechanically speaking, Stroma is the most important layer comprising bundles of collagen fibrils, which provide most of corneal mechanical and optical characteristics [3].

In order to understand how the corneal surgery works, it is essential to study its mechanical behavior, when submitted to external actions. Finite Element Method (FEM) is a numerical tool that allows investigating different surgical techniques, and also understanding the drawbacks of each surgical procedure [2–5].

In order to perform the numerical research, previous calculations must be performed for preparing the computational model.

Firstly, a physical model of the mechanical response of cornea has to be chosen. Once the model has been selected, its parameters have to be calculated running the model to fit experimental data, normally a stress – strain curve.

It is also fundamental to study the corneal geometry used in the modeling, because its form and the boundary conditions influence the outcome of the numerical method.

In order to run the numerical model, a mesh must be selected that guarantees a fast convergence of the procedure and enough precision in the results for an adequate comparison with experimental data.

To complete the task, a stress free configuration of the cornea must be calculated [4].

The present contribution summarizes the results of the first stage of a research performed at the request of the Cuban Institute of Ophthalmology “Ramón Pando Ferrer”. The aim of the research is to create a computational model of a human cornea suitable for medical research. Present stage intends to create the computational model.

The objectives are:

- Using published data [5] of stress – strain in human corneas, to compare the performance of two mechanical models, Mooney – Rivlin of five parameters (MR5)

and Ogden of three parameters (Og3) to predict the refractive power of cornea in different situations.

- Finding an optimal mesh for the mechanical modeling.
- To determine the stress free configuration of cornea as starting point to model a cornea at 15 mmHg.
- To study the influence of the boundary conditions, using a cornea fixed by the limbus and a partial ocular globe formed by cornea, limbus ring and part of sclera.

FEM calculations were performed in ANSYS 18.1.

II. MATERIALS AND METHODS

Corneal elasticity: Corneal tissue shows a highly nonlinear behavior [6] but in a range of intraocular pressures (IOP), between 10 and 25 mmHg, the tissue response is quasi linear, allowing to use a simplification. In this case, it is possible to use a hyperelastic model of Stroma [7–9], and consider it as incompressible, due to its high water content [10].

The principal characteristic of a hyperelastic material is the existence of a Helmholtz free energy function ψ per unit of reference volume. In this case the work performed to change the system only depends on its state in the initial and final configurations. For homogeneous materials, ψ depends only on the deformation gradient tensor \mathbf{F} and the Cauchy stress tensor is determined as [11]

$$\sigma = J^{-1} \frac{\partial \psi(\mathbf{F})}{\partial \mathbf{F}} \mathbf{F}^T. \quad (1)$$

Here $J = \det(\mathbf{F})$. This is the constitutive equation of a hyperelastic material. To apply it, you must choose a model for the material, use the energy density function $\psi(\mathbf{F})$ that corresponds, and calculate σ . For isotropic incompressible materials

$$\psi(\mathbf{F}) = \psi_{iso}(\mathbf{C}) - p(J - 1), \quad (2)$$

where \mathbf{C} is the right Cauchy - Green tensor and p is a Lagrange multiplier chosen high enough to warrantee incompressibility ($J \approx 1$). The second Piola - Kirchhoff tensor is

$$\mathbf{S} = 2 \frac{\partial \psi(\mathbf{C})}{\partial \mathbf{C}}. \quad (3)$$

When \mathbf{C} is expressed only through its invariants

$$\mathbf{S} = 2 \left\{ \frac{\partial \psi}{\partial I_1} \frac{\partial I_1}{\partial \mathbf{C}} + \frac{\partial \psi}{\partial I_2} \frac{\partial I_2}{\partial \mathbf{C}} + \frac{\partial \psi}{\partial I_3} \frac{\partial I_3}{\partial \mathbf{C}} \right\}, \quad (4)$$

and

$$\sigma = J^{-1} \mathbf{F} \mathbf{S} \mathbf{F}^T, \quad (5)$$

Using Cauchy tensor and the material properties, it is possible to calculate the system deformations. With the

principal values of Cauchy stress tensor it is also possible to calculate von Mises stress [12]

$$\sigma_M = \sqrt{\frac{(\sigma_1^2 - \sigma_2^2) + (\sigma_2^2 - \sigma_3^2) + (\sigma_3^2 - \sigma_1^2)}{2}}. \quad (6)$$

Two models used frequently to study the human cornea and other biomaterials are Ogden and Mooney Rivlin ones [11].

Ogden model postulates a dependence of the energy density function on the principal stretches $\lambda_1, \lambda_2, \lambda_3$ as [11]

$$\psi(\lambda_1, \lambda_2, \lambda_3) = \sum_{p=1}^N \frac{\mu_p}{\alpha_p} (\lambda_1^{\alpha_p} + \lambda_2^{\alpha_p} + \lambda_3^{\alpha_p} - 3), \quad (7)$$

where μ_p, α_p are constants of the model and N is the order of the model. It has been demonstrated that with $N = 3$ (Og3) is possible to give a very good agreement with experimental data of rubber and biomaterials [11].

Mooney Rivlin model is derived from Ogden, and is expressed in terms of the first two strain invariants I_1, I_2

$$\psi(I_1, I_2) = \sum_{i+j=1}^N C_{ij} (I_1 - 3)^i (I_2 - 3)^j + \sum_{k=1}^{N-1} \frac{1}{d_k} (J - 1)^{2k}. \quad (8)$$

Here d_k are Lagrange multipliers that guarantee incompressibility and C_{ij} are constants of the model. The model with five parameters (MR5, $N = 2$) gives also very good agreement with experimental data

$$\psi(I_1, I_2) = C_{10}(I_1 - 3) + C_{01}(I_2 - 3) + C_{11}(I_1 - 3)(I_2 - 3) + C_{20}(I_1 - 3)^2 + C_{02}(I_2 - 3)^2 + \frac{1}{d}(J - 1)^2. \quad (9)$$

In both models, in order to determine the value of the constants, it is necessary to fit an experimental stress - strain curve.

Boundary conditions: The ocular globe is constituted by the union of cornea and sclera. Both are connected by the limbus, which also has hyperelastic characteristics. It means that can sustain finite deformations. But for modeling cornea, it is possible to consider the limbus as a fixed ring. It is related with the fact that for the inflation tests performed to determine its mechanical properties, the cornea is fixed by a clamp that avoids any displacement of limbus [12].

Another approach is to consider the whole ocular globe, modeling the sclera also as a Mooney Rivlin hyperelastic material [13]. In this case the fixation of the ocular globe could be accomplished by a box of adipose tissue or by the muscles that control and attach the eye [14]. Corneal response will depend on the form of the boundary chosen.

Another important condition that partially determines corneal behavior is the action of IOP. This is normal pressure acting on the Endothelium, with a mean value (for healthy eyes) of 15 mmHg (2000 Pa).

II.1. Selection of the mesh

The selection of an adequate mesh is necessary to guarantee the quality of the results in FEM modeling. In order to achieve it, is important to prepare a mesh with a large density of elements for obtaining exact results.

Unfortunately, an increment in the density of elements is accompanied by an increment in the computational requirements and in the time consumption for obtaining the solution of the model. It is necessary to find an intermediate solution that encompasses high precision and low computational demands. To achieve this result, we have optimized the corneal mesh varying two parameters: the number of element layers in the cross section of the cornea (radial direction) and the number of elements of the corneal principal meridians located in its anterior surface [4].

In both cases the control parameter to evaluate the results is the corneal optical power. To understand this it must be taken into account that the refracting power of cornea is its principal function.

The optimization procedure is as follows: Keeping a constant number of elements in each surface, the optical power is calculated with the computational model of [15] for a cornea composed by different number of layers, starting by one, up to seven.

Once the number of layers is determined, it remains fixed. Then we change the number of elements in the principal meridians. Beginning with five elements in the meridian line from apex to limbus, we increased it up to 23, calculating the optical power for each value.

II.2. Stress free configuration of cornea

To simulate the mechanical behavior of cornea, sometimes the experimental data used to calculate the constants of the model are measured *in vivo*, which means that the structure of the cornea is under the effect of stresses as the IOP, so it is deformed. This deformed configuration is not suitable for mechanical modeling, because when the model applies pressure the corneal structure will show a larger deformation, different from the real one [4].

An approach used to solve this problem is to calculate the stress free configuration, *i. e.* the form that the cornea would show if the IOP is removed [3,4]. It consists in an iterative procedure where normal IOP is applied to the measured deformed configuration X_0 and the resulting deformation is subtracted from X_0 to obtain the first approximation X_1 to the stress free form. This is submitted again to IOP and the resulting configuration is subtracted from X_1 . This difference is subtracted from X_0 to obtain X_2 . This process continues until it converges to a stress free form that after submitted to IOP gives the original configuration X_0 or a configuration that differs from the real one an amount impossible to detect by the human optical system [4].

III. RESULTS AND DISCUSSION

III.1. Selection of the mechanical model

Using the stress – strain curves of [5] in order to determine the parameters of the two material models to be tested, it is possible to reproduce numerically the outcome of an inflation test. The fitting procedure to calculate the parameters is implemented in ANSYS.

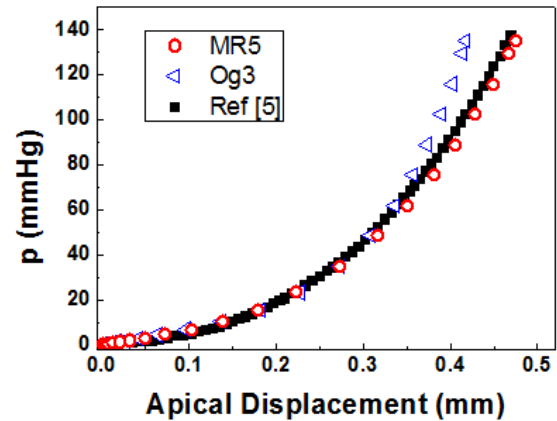


Figure 1. (color online) Deformation response of a human cornea, comparing the prediction of the two models (MR5, red circles, Og3, blue triangles) with the experiments of [5] (full black squares).

Fig. 1 shows the response of the modeled cornea using MR5 and Og3 as compared with experimental results [5].

The abscissa is the apical displacement, defined as the total displacement of the apical point of anterior surface of cornea, and the ordinate is the pressure applied to it. The range shown goes far beyond the physiologically attainable pressures, but is good to make the test. The experimental data [5] was obtained from an *in vitro* inflation experiment; that is how the large range of pressures was obtained. In experimental *in vivo* studies values between 10 and 30 mmHg has been found [16].

From this figure it is possible to see that MR5 reproduces better the experimental data, when pressures from 0 to 140 mmHg are considered. It also occurs in the physiologically important range from 10 to 40 mmHg. To check this, the distance between our calculations and [5] data was determined using the L^2 norm. The results confirm the visual appreciation: in the whole range of pressures $L^2[Exp - Og3] \approx 7L^2[Exp - MR5]$. If we restrict calculations to pressures below 40 mmHg, results are closer, but again $L^2[Exp - Og3] > L^2[Exp - MR5]$. We are interested in a model that describes the deformation response of human cornea at any pressure so, in what follows, MR5 will be used.

III.2. Formulation of the Finite Element model

In Fig. 2 the relative variation of the refractive power with the number of layers in the cross section of cornea is shown.

A fast decrement of the error is observed, and then the value stabilizes in the interval from three to five layers (around

$7 \cdot 10^{-5}$). So, in spite of the ulterior decrement of error, three layers are enough for achieving a good precision in the value of refractive power.

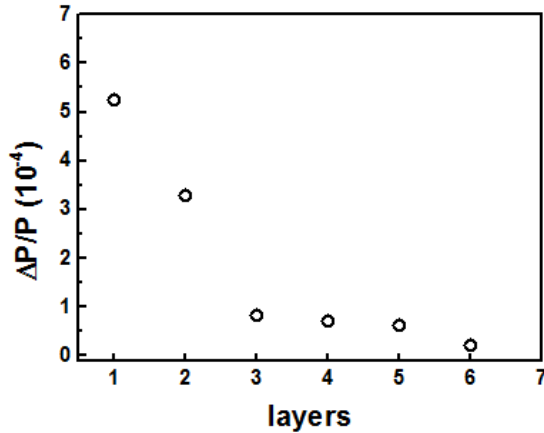


Figure 2. Relative variation of the corneal power with the increase of the number of layers in the cross section.

Similar behavior is obtained in the analysis of the dependence of the relative error of pressure with the number of elements in the half meridians, Fig. 3.

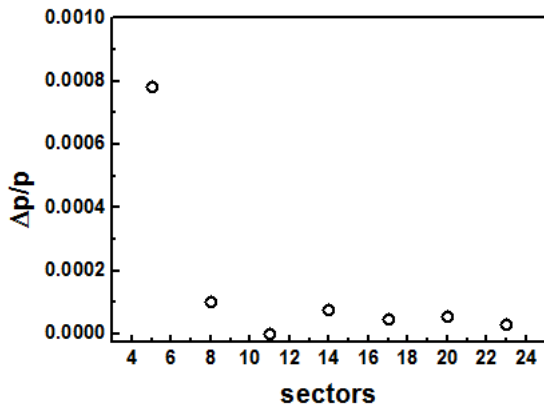


Figure 3. Relative variation of the corneal power with the increase of the number of sectors in the meridians.

When the number of elements changes from five to eight, the error diminishes one order of magnitude; ulterior changes (up to 23) provoke small reductions. At 11 layers the relative change of pressure reaches its minimum and this is the number of sectors selected.

Once determined the mesh, the stress free configuration was obtained.

The calculations for determining the stress free configuration included seven iterations. After each iteration, the refractive power of cornea was determined using the curvature of both surfaces [15].

Fig. 4 (a) shows the dependence of the power P in diopters with the iteration number.

It is easy to observe that after four iterations the corneal configuration is almost equal to the reference value of the corneal form (X_0 , red horizontal line), according to

its refractive power. The convergence of the power to the reference value seems to be exponential.

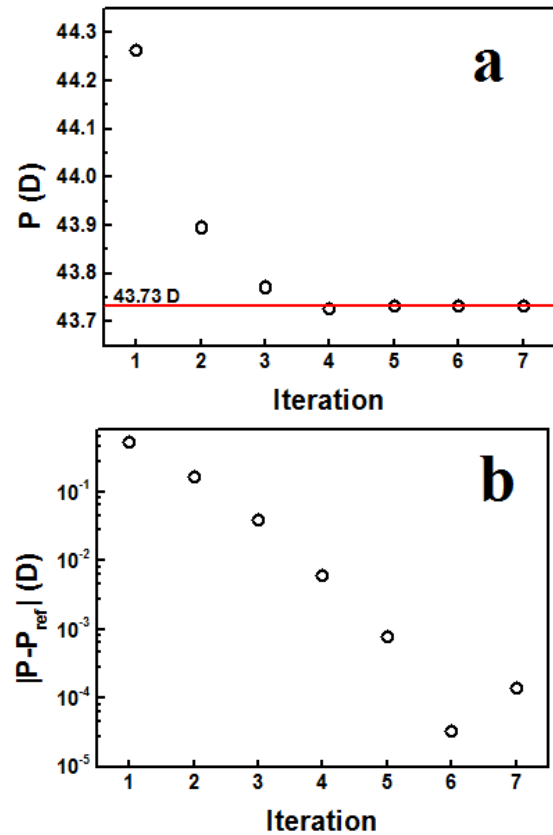


Figure 4. (color online) Variation with the iteration number of (a) the refractive power of cornea and (b) the absolute variation of the refractive power when compared with the reference value of 43.73 D (red horizontal line in (a)). To better appreciate the whole curve a semilog graph is used in (b).

In Fig. 4 (b) the absolute value of the difference between the corneal power in a given iteration and the reference value is plotted against the iteration number in norm – log form. The exponential form of the dependence is clearly observed. After four iterations the difference is around 0.006 D, impossible to detect in a real human eye. So, four iterations seem to be an adequate number to obtain a corneal stressed form close to the real one.

Though these results converge slower than those of [4], the obtained stressed configuration is good enough to follow the preparation of the model.

We finally made the choice between the two boundary conditions. The selection mechanism consists in calculate the response of the two models (with the characteristics determined above) to increases in the values of applied pressure.

The cornea used in the calculations is shown in Fig. 5, where a normal pressure has been applied.

Maximum displacement is obtained in the central part of cornea, while in limbus the displacement is zero, due to the fixed boundary.

The consequence is the increment in the curvature

(diminishment of radius of curvature) which, of course, influences the refractive power of cornea.

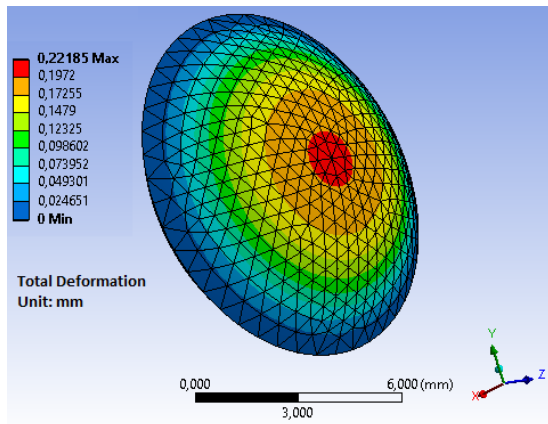


Figure 5. Total displacement of cornea used in the calculations, with normal pressure applied. The effect of the boundary condition provokes a zero displacement in limbus.

The second boundary condition is the partial ocular globe shown in Fig. 6.

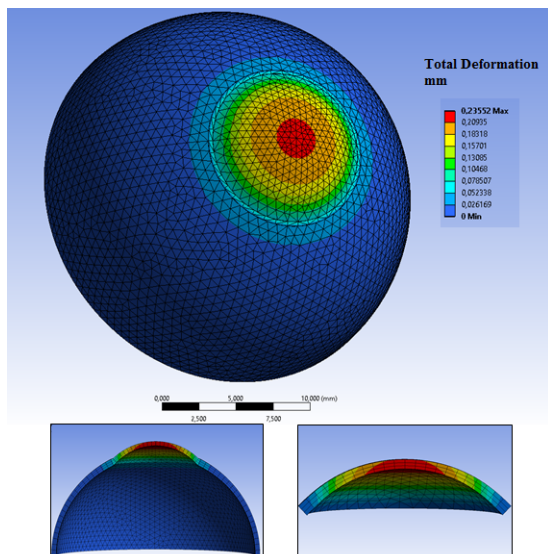


Figure 6. Total displacement of the partial ocular globe, with normal pressure applied. Two sections are shown to better appreciate the displacement distribution.

Differently from Fig. 5, in this case both limbus and sclera suffer certain displacement, which absorb part of the deformation and so, cornea has a different cross section. The overall distribution is better appreciated in the two sections shown in the inferior part of Fig. 6.

The differences in both situations would be reflected in different optical and mechanical behavior when we compare the two systems. The magnitudes selected for investigating these differences are the refractive power of the cornea and the apical displacement.

Figure 7 shows the result obtained for both magnitudes with variations of the IOP from 10 to 40 mmHg.

In figure 7(a) the changes in refractive power show great differences between both models. While cornea alone

increases appreciably its power – from 43 to 45 D – due mainly to the increase of its curvature, the cornea attached to part of the ocular globe shows a slight decrement.

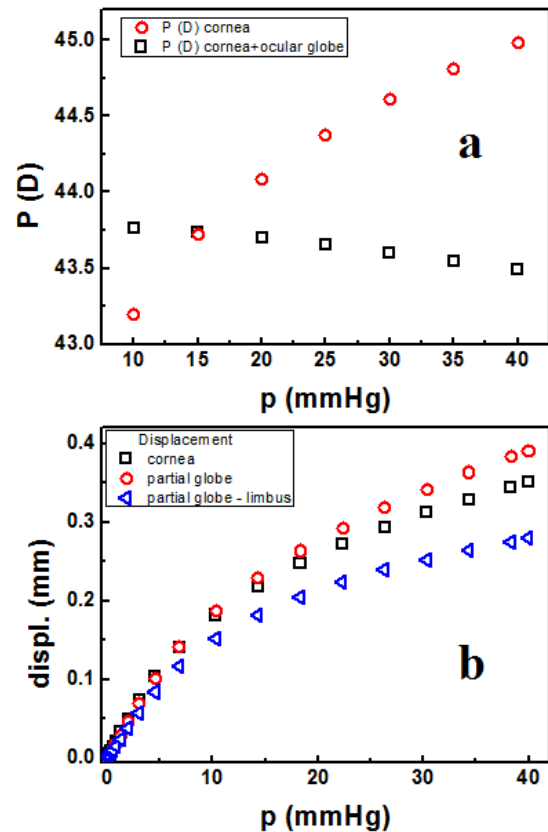


Figure 7. (color online) Effect of IOP on the response of the two corneal models considering (a) refractive power of cornea and (b) the apical displacement. In (b) blue triangles correspond to the displacement of cornea relative to limbus.

This is associated with the redistribution of loads to sclera, which keeps the curvature almost constant. It is easy to see that both systems have the same power at 15 mmHg; this is the reference configuration for both of them.

To understand these results we plot the apical rise vs. IOP in Fig. 7(b). Surprisingly, the apical rise is larger for the partial globe, while for the cornea this rise is smaller. This is counterintuitive if we consider Fig. 7(a) and the idea that the ocular globe is more stable than cornea.

In order to understand this apparent contradiction, we plotted also the apical displacement of cornea relative to limbus (blue triangles in Fig. 7(b)). Now the displacement is smaller, indicating smaller deformation of cornea.

The reason is that in the ocular globe the deformations are transmitted to sclera and limbus, which absorb part of the load as a lateral displacement, leading to lower apical rise and smaller changes of corneal radiuses. Results of Fig. 7 are consistent with the optical stability of human eye in the interval of physiological pressures.

Anyway, we found a nonzero displacement of cornea in the partial globe, but no change in its refractive power. This indicates that only the apical displacement is not indication

of the change in refractive power, being the change of the entire cornea what determines its optical performance. This suggests that for determining the biomechanical constants of cornea, apical rise would give incomplete information. This will be analyzed in future work.

IV. CONCLUSIONS

The biomechanical model of a human cornea consists of a Mooney Rivlin 5 hyperelastic energy density function, the parameters of which are easily determined from experiments, inflation tests for instance. The geometry is composed by cornea, limbus ring and part of sclera, which gives more stability in the corneal response to variations of IOP, and other external influences, making the model response closer to the one expected from a real eye. The mesh used consists of three layers with 11 elements in each half meridian, giving a total of 2 196 elements for cornea and 15 276 for cornea plus part of sclera. In the second case, the number of elements pertaining to cornea is the same as in the first case (2 196).

This model will be applied in the simulation of a LASIK corrective surgery, using parameters obtained from inflation tests performed by us.

V. ACKNOWLEDGEMENTS

Authors thank Prof. David Fernández-Rivas (University of Twente) for his support with the calculations. We also thank Taimí Cárdenas Díaz (MD, PhD) and Iván Hernández López (MD, MSc) (Cuban Institute of Ophthalmology) for useful discussions and suggestions during the preparation and development of the research.

REFERENCES

- [1] I. Simoni and A. Pandolfi, PLoS ONE **10**(6), e0130426 (2015).
- [2] I. Seven, A. S. Roy and W. Dupps, J. Cataract. Ref. Surg. **40**, 943 (2014).
- [3] A. Pandolfi and G. A. Holzapfel, J. Biomech. Eng. **130**, 061006 (2008).
- [4] A. Elsheikh et al., Med. Eng. Phys. **35**, 211 (2013).
- [5] A. Elsheikh et al., Current Eye Res. **32**, 11 (2007).
- [6] J. Dias et al., Exp. Eye Res. **138**, 1 (2015).
- [7] T. Mohammad Nejad, C. D. Foster and D. Gongal, Arq. Bras. Oftalmol. **77**, 60 (2014).
- [8] R. Grytz and G. Meschke, Biomech. Model Mechanobiol. **9**, 225 (2010).
- [9] D. S. Schultz et al., Investig. Ophthalmol. Vis. Sci. **49**, 4232 (2008).
- [10] R. M. Torres, J. Merayo-LlLoves, M. A. Jaramillo and V. Galvis, Arch. Soc. Esp. Oftalmol. **80**, 215 (2005).
- [11] G. A. Holzapfel, Non-linear solid mechanics: a continuum approach for engineering. (John Wiley & Sons, New York, USA, 2000).
- [12] K. Anderson, A. El-Sheikh and T. Newson, J. R. Soc. Interface **1**, 3 (2004).
- [13] A. Elsheikh et al., Exp. Eye Res. **90**, 624 (2011).
- [14] I. Sigal, J. G. Flanagan and C. R. Ethier, Investig. Ophthalmol. Vis. Sci. **46**, 4189 (2005).
- [15] C. Muñoz-Villaescusa, O. Núñez-Chongo and A. J. Batista-Leyva, Rev. Cubana Fis. **31**, 35 (2014).
- [16] H. H. Cagatay et al., The Scientific World Journal **2014**, 11 (2014).

This work is licensed under the Creative Commons Attribution-NonCommercial 4.0 International (CC BY-NC 4.0, <http://creativecommons.org/licenses/by-nc/4.0>) license.

